Available online at www.sciencedirect.com
ScienceDirect
Tetrahedron 64 (2008) 1397–1408
Tetrahedron
www.elsevier.com/locate/tet

The alkaloids of the mersinine group: a new subclass of the monoterpenoid indole alkaloids from *Kopsia*

G. Subramaniam [a,†], Yeun-Mun Choo [a,†], Osamu Hiraku [b], Kanki Komiyama [b], Toh-Seok Kam [a,*]

[a] *Department of Chemistry, University of Malaya, 50603 Kuala Lumpur, Malaysia*
[b] *The Kitasato Institute, 5-9-1 Shirokane, Minato-ku, Tokyo 108-8642, Japan*

Received 1 September 2007; received in revised form 29 October 2007; accepted 15 November 2007
Available online 19 November 2007

Abstract

A total of 16 alkaloids, exemplified by mersinine A and its congeners, and constituting a new subclass of the monoterpenoid indoles, were isolated exclusively and for the first time from *Kopsia singapurensis*. The structures of these alkaloids were established by spectroscopic methods and in some instances confirmed by X-ray diffraction analysis. A possible biogenetic route from an aspidofractinine precursor is proposed. Compounds **1**, **2**, **3**, **9**, and **10** were found to reverse multidrug-resistance in drug-resistant KB cells.

Keywords: Alkaloids; NMR; *Kopsia*; Plants

1. Introduction

Plants of the genus *Kopsia* (Apocynaceae) continue to provide novel indole alkaloids with intriguing carbon skeletons.[1–21] Recent examples of unusual alkaloids from *Kopsia*, which are notable for possessing novel ring systems include, inter alia, the cage indole arbophylline,[3] the three-nitrogen pentacyclic indole arboflorine,[4] the tetracyclic indole mersicarpine,[6] the tetracyclic quinolinic alkaloid, mersilongine,[7] and the regioisomeric tetracyclic indoles, arboricine and arboricinine.[1] We previously reported the isolation and structure elucidation of mersinines A and B and mersiloscine from the leaf extract of *Kopsia singapurensis*.[10] We now report in full the isolation and structure determination of 13 other alkaloids of the same structure type isolated from the same plant.[22,23]

These new alkaloids are characterized by a novel pentacyclic skeleton incorporating a quinolinic chromophore, and are encountered exclusively and for the first time from the same plant. From a biogenetic viewpoint, these compounds may be envisaged to have arisen from an aspidofractinine precursor via formation of an aziridinium intermediate, followed in succession by aziridinium ring opening and reduction as shown in Scheme 1 (in analogy to the route used by Levy for a biomimetic entry into the *Melodinus* alkaloids, scandine and melo-

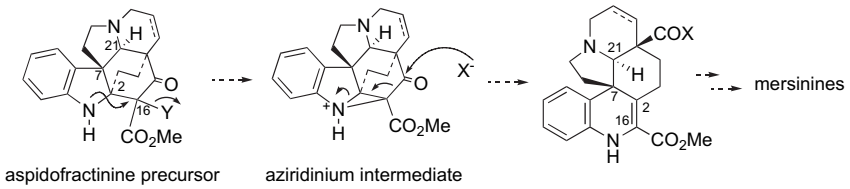

Scheme 1.

* Corresponding author. Tel.: +60 3 79674266; fax: +60 3 79674193.
E-mail address: tskam@um.edu.my (T.-S. Kam).
† Present address: MerLion Pharmaceuticals, 1 Science Park Road, The Capricorn 05-01, Singapore Science Park II, Singapore 117528, Singapore.

0040-4020/$ - see front matter © 2007 Elsevier Ltd. All rights reserved.
doi:10.1016/j.tet.2007.11.047

scine).[24,25] The proposed pathway leads to the numbering system adopted for the alkaloids of this new subclass.

2. Results and discussion

Mersinines A (**1**) and B (**2**) have essentially the same structure and share many spectral features.[10] Both showed the same molecular ion in EIMS at *m/z* 500 indicating that they are isomers. The UV spectra of both were similar with absorption maxima (e.g., 213, 239, and 289 nm for **1**) characteristic of a tetrahydroquinoline chromophore. Both compounds possess OH, ester, and carbamate functions as indicated by the IR, ^{1}H, and ^{13}C NMR spectral data (See Section 3 and Tables 1 and 3). Analysis of the NMR spectral data (COSY, HMQC, HMBC) of both alkaloids (Fig. 1, HMBCs of **1**) led to the pentacyclic quinolinic structures as shown in **1** and **2**.[10] The relative configurations at C-21 and C-2 were established from NOE experiments. Thus irradiation of H-9 resulted in enhancement of the H-21 signal, while irradiation of H-21 in turn caused enhancement of H-9 as well as H-2, allowing the stereochemistry of H-2 and H-21 to be assigned as α. Other observed NOEs (Fig. 2) include those from H-19α to H-2 and H-21. The main difference in the structure of **1** and **2** lies in the configuration of the quaternary center, C-16. The first indication of such an epimeric relationship was provided by the observation that mersinine A (**1**) was smoothly and irreversibly converted to mersinine B (**2**) by the action of dilute alcoholic NaOH, indicating that compound **2** was the more stable epimer.[10] Examination of molecular models confirmed that the less sterically congested structure has the hydroxyl substituent in the β-position. This difference in the stereochemistry at C-16 was also reflected in differences in the NMR spectral data between **1** and **2**, which involve the resonances of H-6, C(16)–OH, and C-2. Compound **2** and others with similar 16(*S*) configuration in the mersinine series (vide infra) showed strikingly similar C(16)–OH shifts in ^{1}H NMR (ca. *δ* 5.1), which are distinct from the C(16)–OH shifts in compound **1** and others with opposite, i.e., 16(*R*) configuration (ca. *δ* 4.6). A similar trend was indicated in the carbon shifts of C-2 (ca. *δ* 49 in **2** cf *δ* 53 in **1**). Additional support for this assignment was provided by the paramagnetic deshielding of H-18 (α or β) by the proximate C(16)–OH group.[26,27] The stereochemistry of the C-18 hydrogens can be independently assigned through consideration of the vicinal coupling constants and from NOE experiments. In compound **1**, in which the C(16)–OH group is α, H-18α experiences deshielding due to spatial proximity of the α-oriented OH (H-18α *δ* 1.78, H-18β *δ* 1.34), whereas in compound **2**, the same effect operates on H-18β instead, which was deshielded to ca. *δ* 1.8 (H-18α ca. *δ* 1.3).[26,27] These conclusions have been subsequently confirmed by an X-ray analysis of mersinine A,[28] which also confirmed the assignment of the relative configurations at the various stereocenters of **1** and **2** based on NOE data.[10]

Mersinine C (**3**) was obtained as colorless crystals, mp 108–110 °C, $[\alpha]_D$ +14 (*c* 0.72, $CHCl_3$). The UV spectrum was similar to that of **1** and **2**, as was the IR spectrum, which showed bands due to OH, ester, and carbamate functions. The IR spectrum, however, showed two additional (Wenkert–Bohlmann) bands at 2782 and 2874 cm^{-1}, which were not seen in the case of **1** and **2**. The EIMS showed the same molecular ion at *m/z* 500 indicating that mersinine C is isomeric with **1** and **2**. The ^{1}H and ^{13}C NMR spectral data (Tables 1 and 3, respectively) were also generally similar, except for changes in several of the chemical shifts, as were the COSY and HMBC data, indicating affinity with the previous two compounds. In common with both **1** and **2**, the C-7 and C-21 configurations are defined by the observed reciprocal NOEs for H-21 and H-9, while the observed C(16)–OH shift at *δ* 5.13 as well as the deshielding of H-18β relative to H-18α, are diagnostic of an 16(*S*) configuration as described for mersinine B (**2**) (vide supra). In contrast to **1** and **2**, however, the H-21/H-2 NOE was not observed (Fig. 3), although the observed H-18β/H-6β NOE in this case allowed the stereochemistry of H-2 to be assigned as α. The C-2 resonance at *δ* 44.1, however, was not consistent with the trend observed for the other two alkaloids and in addition, several other NOE interactions, such as those between H-21/H-19α and H-2/H-19α, which were observed for **1** and **2**, were conspicuously not observed in mersinine C (**3**). These departures can be rationalized, not only by the change in the D/E ring junction stereochemistry from cis as in mersinines A and B, to trans in mersinine C, with H-21 and the *N*(4) lone pair oriented *anti* to each other as indicated by the observed Wenkert–Bohlmann bands in the IR spectrum of **3**,[29,30] but also by the change in the configuration at C-20 from *R* to *S*. The observed NOE data become intelligible on the basis of this structure. Examination of models showed that H-2 and H-19α are no longer proximate to H-21 in mersinine C. Mersinine C represents the first member of this sub-group of which there are three others (vide infra), which are characterized by the presence of a trans-D/E ring junction and C(20)–αCO_2Me.

Three other alkaloids (**4**–**6**), characterized by incorporation of an additional lactone ring, were also obtained. Mersiloscine (**4**) showed a molecular ion at *m/z* 502 by EIMS, which analyzed for $C_{24}H_{26}N_2O_{10}$ (DBE 13). The ^{1}H and ^{13}C NMR spectral data of **4** (Tables 1 and 3) showed a basic similarity with those of compounds **1** and **2** except for some notable differences consistent with the formation of a γ-lactone unit incorporating C-14, C-15, C-20, and C-17, and the presence of an OH substituent at C-15.[10] This proposal is also supported by the observed three-bond correlations from H-14 and H-21 to the lactone carbonyl (C-17) in the HMBC spectrum of **4**. Another significant difference is the downfield shift of H-18β from *δ* 1.85 in **2** to *δ* 3.02 in **4**, which is caused by the anisotropic effect of the proximate lactone carbonyl function. This observation allowed the assignment of the C-20 to C-17 bond as β, since the alternative structure (in which the lactone unit is α with respect to the general plane defined by the molecule) would result in the placement of H-19α instead, within the anisotropic influence of the lactone carbonyl function. On the assumption that the lactone **4** is formed from a hypothetical hydroxy ester/acid precursor such as **7**, which is in turn derived from oxidation of the olefin **2**, it would be reasonable to conclude that the stereochemistry of the ester group at

Table 1
^{1}H NMR spectral data of **1**–**6** and **8**–**9**[a]

H	**1**	**2**	**3**	**4**	**5**	**6**	**8**	**9**
2	2.14 dd (13, 3)	2.08 dd (13, 3)	1.91 m	1.96 dd (13, 3)	1.97 dd (13, 3)	1.97 dd (13, 3)	2.55 dd (13, 3)	2.52 dd (13, 3)
3α	3.97 dd (18, 5)	4.05 dd (18, 5)	3.02 br d (16)	3.60 d (15)	3.55 d (15)	3.37 m	4.05 dd (18, 5)	4.04 dd (18, 5)
3β	3.57 ddd (18, 3, 2)	3.60 ddd (18, 3, 2)	3.55 dd (16, 5)	3.10 dd (15, 3)	3.04 dd (15, 3)	3.37 m	3.66 m	3.65 m
5α	3.11 m	3.18 m	2.26 ddd (12.5, 8, 5)	3.20 m	3.16 m	3.23 m	3.14 m	3.12 m
5β	2.98 t (8.5)	3.09 t (8.5)	3.04 m	3.20 m	3.16 m	3.23 m	3.14 m	3.12 m
6α	1.62 dd (12.5, 6.5)	1.57 dd (12.5, 6.5)	1.57 dd (12.5, 5)	1.63 m	1.66 m	1.67 dd (14, 6.5)	1.47 dd (12.5, 6.5)	1.45 dd (12.5, 6.5)
6β	1.99 m	2.33 m	2.87 td (12.5, 7)	2.81 ddd (13.5, 10.5, 9.5)	2.61 m	2.80 m	2.20 dt (12.5, 9.5)	2.15 dt (12.5, 9.5)
9	7.15 d (8.2)	7.18 d (8.2)	6.94 d (8.2)	7.20 d (8.2)	7.16 d (8.2)	7.06 d (8.2)	7.62 d (7, 1.5)	7.52 d (8.5)
10	6.62 d (8.2)	6.62 d (8.2)	6.61 d (8.2)	6.62 d (8.2)	6.64 d (8.2)	6.60 d (8.2)	7.06 m	6.62 d (8.5)
11	—	—	—	—	—	—	7.03 m	—
14	5.95 ddd (9.5, 5, 2)	5.97 ddd (9.5, 5, 2)	5.78 br dd (9.5, 5)	4.46 dd (5.5, 3)	4.43 dd (5.5, 3)	4.54 br s	5.97 ddd (9.5, 5, 2)	5.97 ddd (9.5, 5, 2)
15	5.82 dd (9.5, 3)	5.86 dd (9.5, 3)	5.67 br d (9.5)	4.27 d (5.5)	4.21 d (5.5)	3.98 s	5.88 br dd (9.5, 3)	5.88 dd (9.5, 3)
18α	1.78 dq (13, 3)	1.33 br d (13)	1.50 ddt (13.5, 10, 3.5)	1.30 m	1.66 m	1.33 m	1.36 dq (13, 3)	1.32 m
18β	1.34 br q (13)	1.85 qd (13, 3)	2.13 m	3.02 qd (13, 3)	2.33 qd (13, 3)	2.94 qd (13, 3)	1.88 qd (13, 3)	1.87 qd (13, 3)
19α	1.16 td (13, 3)	1.16 td (13, 3)	2.34 ddd (13.5, 10, 8)	1.33 td (13, 3)	1.31 td (13, 3)	1.19 td (13, 3)	1.23 m	1.22 td (13, 3)
19β	2.39 dt (13, 3)	2.42 dt (13, 3)	1.89 m	1.63 m	1.58 dt (13, 3)	2.15 dt (13, 3)	2.50 dt (13, 3)	2.48 m
21	3.00 s	3.09 s	3.55 s	3.73 s	3.63 s	2.99 s	3.21 s	3.16 s
17-OMe	3.63 s	3.66 s	3.46 s	—	—	—	3.67 s	3.67 s
22-OMe	3.82 s	3.80 s	3.79 s	3.80 s	3.78 s[b]	3.80 s[c]	3.91 s	3.91 s
NCO_2Me	3.79 s	3.80 s	3.79 s	3.81 s	3.88 s[b]	3.84 s[c]	—	—
OCH_2O	5.91 d (1.5)	5.92 d (1.5)	5.96 br s	5.92 d (1.5)	5.90 br s	5.93 d (1.5)	—	—
	5.96 br s	5.96 d (1.5)	5.96 br s	5.95 br s	5.97 br s	5.97 br s	—	—
16-OH	4.61 br s	5.08 br s	5.13 br s	5.08 br s	4.75 br s	5.08 br s	4.71 br s	4.72 br s
15-OH	—	—	—	2.45 br s	3.24 br s	—	—	—
11-OMe	—	—	—	—	—	—	—	3.99 s

[a] $CDCl_3$, 400 MHz; assignments based on COSY and HMQC.
[b,c] Assignments may be reversed.

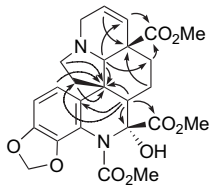

Figure 1. Selected HMBCs of **1**.

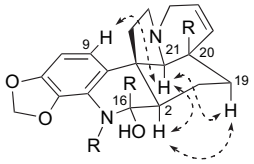

Figure 2. Selected NOEs of **1** (R=CO_2Me).

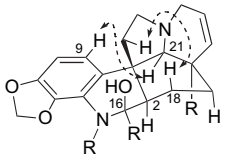

Figure 3. Selected NOEs of **3** (R=CO_2Me).

C-20 in these closely related compounds (**1**, **2**, **4**–**7**) is β. Irradiation of H-21 caused enhancement of H-19α (in addition to H-2 and H-9). Irradiation of H-19β in turn caused enhancement of H-15 and vice versa, from which the stereochemistry of the C(15)–OH can be established as α. The relative configuration of C-16 was deduced to be similar to that in mersinines B (**2**) and C (**3**), i.e., 16(*S*), from the diagnostic C(16)–OH and C-2 chemical shifts of ca. δ 5.1 and 48, respectively. The β-oriented C(16)–OH group also causes deshielding of H-18β relative to H-18α (δ 3.0 vs 1.3, respectively) but in the case of mersiloscine (**4**), this paramagnetic deshielding due to OH is reinforced by additional deshielding from anisotropy of the lactone carbonyl. Mersiloscine A (**5**) was readily deduced to be the C-16 epimer of mersiloscine (**4**) from the spectral data, which were in all respects similar to those of **4**, except for the diagnostic C(16)–OH and C-2 chemical shifts (δ 4.75 and 51.8, respectively), which were indicative of a 16(*R*) configuration. Similarly the spectral data for mersiloscine B (**6**) indicated similarity with mersiloscine (**4**), except for differences in the shifts of H-19β and H-21, and C-3, C-14, C-15, C-19, C-20, and C-21. The main difference in mersiloscine B (**6**) compared to mersiloscine (**4**) concerns the stereochemistry of the C(15)–OH substituent, which can be inferred from NOE experiments. Thus irradiation of H-15 resulted in enhancement of H-21 and vice versa, but had no effect on H-19β. This observation allowed the assignment of the stereochemistry of the C(15)–OH group as β. Mersiloscine B (**6**) is therefore 15-*epi*-mersiloscine.

Three mersinine-type alkaloids (mersifolines A–C, **8**–**10**) characterized by incorporation of an unprecedented oxazoloquinoline chromophore were also obtained. Mersifoline A (**8**) was obtained as a colorless oil with $[\alpha]_D$ −19 (*c* 0.26, $CHCl_3$). The UV spectrum (λ_{max} 206, 230, and 271 nm) was essentially similar to that of the previous compounds in the mersinine series, indicating the presence of the same tetrahydroquinoline chromophore. The IR spectrum showed bands at 3434, 1784, and 1738 cm^{-1}, indicating the presence of OH, five-membered cyclic carbamate, and ester functionalities, respectively. The ^{13}C NMR spectrum (Table 3) showed a total of 23 signals comprising two methyls, five methylenes, seven methines, and nine quaternary carbons. The spectrum also indicated the presence of carbamate (δ 152.1) and two ester functions (δ 170.3, 173.4). The ^{1}H NMR spectrum (Table 1) showed the presence of three contiguous aromatic hydrogens (δ 7.61, 7.06, 7.03), two methoxy groups associated with the ester functions (δ 3.67, 3.91), a 14,15-double bond (δ 5.88, 5.97), and an OH function (δ 4.71). The COSY spectrum showed the same partial structures that are present in the mersinines (**1**–**3**), i.e., NCH_2CH_2, $NCH_2CH{=}CH$, and CH_2CH_2CH, and the essentially similar HMBC data indicated that the carbon skeleton was essentially unchanged. The observation of characteristic reciprocal NOEs for H-9/H-21, H-21/H-19α, H-21/H-2, and H-2/H-19α, coupled with the similarity of the NMR spectral data, indicated that the configurations at C-7, C-21, C-2, and C-20 are similar to those of mersinines A and B. The H-9/H-21 NOE indicated that substitution of the aromatic ring is at C-12 and the observed carbon resonance of C-12 at ca. δ 141 was suggestive of some form of oxygenation. However, although a carbamate function was indicated by the ^{13}C NMR spectrum (δ 152.1), the corresponding methyl resonance was conspicuously absent and moreover the molecular formula for mersifoline A (DBE 13) requires the formation of an additional ring. These features taken together indicated the formation of a cyclic carbamate in which the oxygen of the carbamate function is linked to the aromatic C-12, furnishing an oxazoloquinoline structure as shown in structure **8**. This conclusion receives additional support from the unusual IR band at 1784 cm^{-1}, which has been noted previously (1780 cm^{-1}) for such oxazoloquinoline class of compounds.[31] The mersifolines (**8**–**10**) represent the first examples of an indole or indole-derived alkaloid incorporating such a functionality. In the case of the mersifolines, the C(16)–OH resonance was observed at ca. δ 4.7 in all three compounds (**8**–**10**), suggesting a similar configuration in all three compounds. The shift of C-2 at δ 48.8 in mersifoline A (**8**) is diagnostic of a 16(*S*) configuration, and this conclusion was further supported by the observed deshielding of the H-18β resonance compared to that of H-18α, due to the proximate, β-oriented C(16)–OH group. It would appear that the replacement of the usual carbamate substituent on the indolic nitrogen by a cyclic carbamate unit has resulted in a change in the C(16)–OH resonance, which has been shifted upfield from the normal value of ca. δ 5.1 for mersinine-type compounds with 16(*S*) configuration.

Mersifoline B (**9**) was obtained as a colorless oil with $[\alpha]_D$ −14 (*c* 0.18, $CHCl_3$). The UV spectrum was essentially similar to that of mersifoline A (**8**). The IR spectrum was also similar showing bands due to OH (3463 cm^{-1}), five-membered cyclic carbamate (1781 cm^{-1}), and ester carbonyls (1735 cm^{-1}), which were also common in **8**. With the exception of the aromatic resonances, the ^{1}H and ^{13}C NMR of mersifolines B and A were almost similar, as were the COSY, HMBC, and NOE

data, indicating a similar ring system as well as similar relative configuration at the various stereogenic centers. The mass spectrum (M^+ *m/z* 470) gave a different molecular formula compared with that of mersifolines A (**8**) and C (**10**), differing by 30 mass units (replacement of H by OMe). The ^{1}H NMR spectrum showed (Table 1) a pair of AB doublets in the aromatic region (δ 6.62, 7.52) and this coupled with the ^{13}C NMR spectrum (Table 3), and the presence of an additional aromatic methoxy signal (δ 3.99) in addition to two others due to the methyl ester functions (δ 3.66, 3.91), confirmed the presence of a methoxy substituent at C-11. The structure of mersifoline B is therefore as shown in **9**.

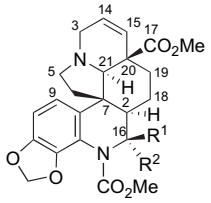

1 $R^1 = CO_2Me$, $R^2 = OH$
2 $R^1 = OH$, $R^2 = CO_2Me$

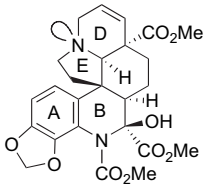

3

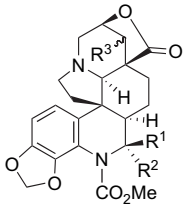

4 $R^1 = OH$, $R^2 = CO_2Me$, $R^3 = \alpha$-OH
5 $R^1 = CO_2Me$, $R^2 = OH$, $R^3 = \alpha$-OH
6 $R^1 = OH$, $R^2 = CO_2Me$, $R^3 = \beta$-OH

Mersifoline C (**10**) was obtained as a colorless oil with $[\alpha]_D$ +18 (*c* 0.28, $CHCl_3$). The UV spectrum was essentially similar to that of mersifolines A (**8**) and B (**9**). The mass spectrum (M^+ *m/z* 440) was similar to that of mersifoline A (**8**), indicating that **10** and **8** were isomers. The IR spectrum was also similar showing bands due to OH (3468 cm^{-1}), five-membered cyclic carbamate (1784 cm^{-1}), and ester carbonyls (1752, 1728 cm^{-1}), which were also common in **8** and **9**. However, unlike mersifoline A (**8**), two additional bands at 2791 and 2874 cm^{-1} (Wenkert–Bohlmann bands) were also observed in the IR spectrum of **10**, which provided the first indication that mersifoline C resembles mersinine C (**3**), in having a trans-D/E ring junction and a 20(*S*) configuration (C(20)–αCO_2Me). This was further confirmed on examination of the NMR spectral data (Tables 2 and 3), which showed departure of some of the ^{1}H and ^{13}C chemical shifts when compared with those of mersifoline A (**8**). The COSY and HMBC data were, however, similar, indicating the presence of a similar ring system. The characteristic C(16)–OH at δ 4.70, as well as the deshielding of H-18β relative to H-18α, is diagnostic of an *S* configuration at C-16, as is the case in mersifolines A (**8**) and B (**9**). However, unlike compounds **8** and **9**, the C-2 resonance in **10** was shifted upfield to ca. δ 42, which is similar to the situation in mersinine C (**3**), as a consequence of changes in both the D/E ring junction stereochemistry as well as that of the C(20)–methyl ester group. The NOESY/NOE data of mersifoline C (**10**) were also similar to those of mersinine C (**3**), in that while the H-21/H-19α, H-21/H-2, and H-2/H-19α NOEs were not observed, the H-9/H-21, H-18β/H-6β, and H-3α/H-21 NOEs were seen. These observations, coupled with the similarity of the NMR spectral data with those of mersinine C, are consistent with a structure with a trans-D/E ring junction and an (*S*) configuration at C-20 (C(20)–αCO_2Me). The structure of mersifoline C is therefore as shown in **10**. The mersifolines are distinguished by the presence of the unprecedented oxazoloquinolinic chromophore in an indole (or indole-derived) alkaloid isolated from plants.

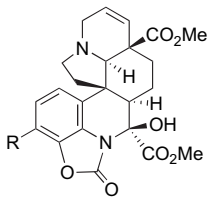

8 R = H
9 R = OMe

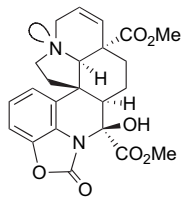

10

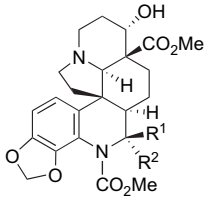

11 $R^1 = CO_2Me$, $R^2 = OH$
12 $R^1 = OH$, $R^2 = CO_2Me$

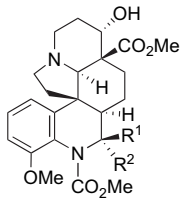

13 $R^1 = CO_2Me$, $R^2 = OH$
14 $R^1 = OH$, $R^2 = CO_2Me$

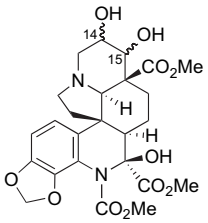

7 14-βOH, 15-αOH
15 14-αOH, 15-βOH

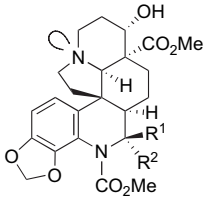

16 $R^1 = CO_2Me$, $R^2 = OH$
17 $R^1 = OH$, $R^2 = CO_2Me$

Table 2
^{1}H NMR spectral data of **10**–**17**[a]

H	**10**	**11**	**12**	**13**	**14**	**15**	**16**	**17**
2	2.30 m	1.99 br d (13)	1.97 m	1.95 dd (13, 3)	1.93 ddd (13, 3, 1.5)	2.02 m	1.77 m	1.70 m
3α	3.26 br d (16)	3.14 dt (12, 4)	3.18 dt (12, 4)	3.18 m	3.17 dt (12, 4)	3.17 dd (13.5, 8.5)	2.58 br t (11)	2.58 br t (11)
3β	3.52 dd (16, 5)	2.55 td (12, 4)	2.63 td (12, 4)	2.58 td (12, 4)	2.61 td (12, 4)	3.55 dd (13.5, 7)	2.91 ddd (11, 5, 1.5)	2.93 br dd (11, 5)
5α	2.58 m	3.06 m	3.10 m	3.08 m	2.96 m	3.04 m	2.27 ddd (12.5, 8, 5)	2.27 m
5β	3.03 m	2.87 m	2.95 m	2.88 m	3.09 m	3.27 t (8.5)	2.83 t (8)	2.86 m
6α	1.50 m	1.59 dd (12.5, 6.5)	1.56 m	1.64 m	1.59 m	1.59 dd (12.5, 6.5)	1.52 dd (12.5, 5)	1.50 m
6β	2.61 m	2.78 m	2.95 m	2.88 m	2.96 m	2.39 dt (12.5, 8.5)	2.63 m	2.84 m
9	7.22 d (8)	7.22 d (8.2)	7.25 d (8.2)	7.35 d (8)	7.35 dd (8, 1)	6.82 d (8.2)	7.13 d (8.2)	7.11 d (8.2)
10	7.11 t (8)	6.62 d (8.2)	6.63 d (8.2)	7.14 t (8)	7.12 br t (8)	6.61 d (8.2)	6.69 d (8.2)	6.66 d (8.2)
11	7.05 d (8)	—	—	6.82 d (8)	6.83 dd (8, 1)	—	—	—
14α	5.84 br dd (9.5, 5)	1.74 m	1.77 m	1.70 m	1.76 m	—	1.68 m	1.70 m
14β	—	2.26 ddt (14.5, 7.5, 4)	2.26 ddt (14.5, 7.5, 4)	2.27 ddt (14.5, 7.5, 4)	2.26 ddt (14.5, 7.5, 4)	3.91 m	2.12 m	2.15 m
15	5.62 br d (9.5)	4.41 dd (7.5, 6)	4.40 dd (7.5, 6)	4.42 dd (7.5, 6)	4.41 dd (7.5, 6)	3.34 d (8.5)	3.83 m	3.85 m
18α	1.43 m	1.71 m	1.32 m	1.70 m	1.32 m	1.34 m	1.76 m	1.48 m
18β	1.98 m	1.06 br q (13)	1.63 br q (13)	1.10 br q (13)	1.64 m	1.83 br q (13)	1.60 m	2.09 m
19α	2.28 m	1.45 td (13, 3)	1.42 td (13, 3)	1.45 td (13, 3)	1.40 td (13, 3)	1.01 td (13, 3)	1.84 m	1.88 m
19β	2.11 ddd (13, 10, 5)	1.92 dt (13, 3)	1.97 m	1.92 m	1.96 m	2.54 dt (13, 3)	2.15 m	2.06 m
21	3.69 s	3.37 s	3.46 s	3.43 s	3.46 s	2.83 s	3.52 s	3.51 s
17-OMe	3.48 s	3.67 s	3.71 s	3.68 s	3.70 s	3.75 s	3.43 s	3.34 s
22-OMe	3.91 s	3.78 s	3.79 s	3.72 s[d]	3.76 s	3.80 s	3.77 s[b]	3.77 s[c]
NCO_2Me	—	3.83 s	3.80 s	3.83 s[d]	3.73 s	3.80 s	3.83 s[b]	3.78 s[c]
OCH_2O	—	5.91 d (1.5)	5.92 d (1.5)	—	—	5.59 br s	5.93 d (1.5)	5.95 br s
	—	5.96 br s	5.95 br s	—	—	5.96 br s	5.97 br s	5.95 br s
16-OH	4.70 br s	4.65 br s	5.11 br s	4.57 br s	5.21 d (1.5)	5.13 br s	4.42 br s	5.13 br s
15-OH	—	—	—	—	—	—	2.01 br s	—
12-OMe	—	—	—	3.83 s	3.82 s	—	—	—

[a] $CDCl_3$, 400 MHz; assignments based on COSY and HMQC.
[b–d] Assignments may be reversed.

Table 3
^{13}C NMR data of **1**–**6** and **8**–**17**[a]

C	1	2	3	4	5	6	8	9	10	11	12	13	14	15	16	17
2	52.9	49.2	44.1	47.9	51.8	48.0	48.5	48.6	41.5	53.1[g]	49.4	53.6	49.6	48.7	49.1	44.5
3	49.6	49.6	52.7	45.2	45.2	50.2	49.6	49.7	51.2	44.2	44.0	44.2	44.0	51.9	46.6	46.6
5	53.8	53.8	52.6	52.1	52.2	52.1	53.2	53.3	51.0	53.2[g]	53.1	53.2	53.2	50.8	52.4	52.5
6	30.4	30.2	32.8	29.7	29.8	29.6	31.5	31.6	34.8	31.7	31.7	31.4	31.2	31.8	33.9	33.2
7	45.6	45.3	44.9	46.1	46.4	46.7	45.0	44.5	44.0	46.2	46.0	46.7	46.4	45.9	44.9	44.9
8	136.6	136.6	134.0	135.1	135.3	134.7	131.3	123.9	130.7	137.6	137.4	[b]	145.5	136.9	134.3	134.0
9	115.8	115.7	115.8	116.5	116.6	116.0	120.0	120.8	118.9	115.7	115.5	115.7	115.6	114.8	117.2	117.1
10	105.1	104.4	103.0	104.4	105.2	104.3	122.6	108.2	122.2	105.1	104.4	126.2	125.4	104.4	103.6	103.0
11	146.8	146.7	146.8	146.8	146.9	147.0	107.8	141.8	107.8	146.2	146.6	110.2	110.4	146.8	146.5	146.3
12	140.2	139.1	139.7	139.0	140.1	139.2	141.0	129.0	141.2	140.2	139.2	152.8	152.2	139.4	140.2	139.2
13	118.0	118.1	119.5	119.0	118.1	119.1	126.0	127.3	125.3	117.8	118.6	123.8	124.7	118.8	118.9	119.3
14	131.7	131.9	124.6	76.7	77.2	80.9	132.0	132.1	126.9	32.3	32.2	32.2	32.3	69.3	29.9	29.7
15	131.9	132.1	131.0	73.0	72.7	82.0	132.1	132.0	130.0	69.3	69.5	69.4	69.7	81.6	70.8	70.8
16	87.6	86.5	86.3	86.5	87.7	86.4	83.6	83.6	82.8	87.4	86.5	87.5	86.2	86.5	88.2	86.4
17	173.0	173.1	175.7	178.6	179.7	178.9	173.4	173.5	175.7	175.1	175.0	175.1	175.1	173.3	176.3	176.5
18	21.5	20.4	16.6	17.3	18.7	17.1	20.6	20.6	16.6	20.5	19.6	20.6	19.6	20.0	17.9	16.4
19	30.9	30.1	26.9	25.7	26.5	22.9	30.6	30.6	25.9	29.3	28.4	29.3	28.5	28.5	24.2	24.0
20	48.6	48.7	47.2	45.6	46.0	49.2	48.8	48.7	48.0	53.4	52.7	52.8	52.7	52.9	50.3	50.3
21	71.5	71.1	65.4	62.1	62.4	70.4	71.4	71.6	66.5	63.3	63.0	63.0	62.7	70.2	63.1	63.1
22	170.5	172.5	172.6	172.8	173.0	172.6	170.3	170.5	170.2	170.5	172.6	170.8	172.6	172.4	170.9	172.7
17-OMe	51.6	51.7	51.9	—	—	—	52.0	52.0	52.1	51.9	51.9	51.9	51.9	51.8	51.7	51.4
22-OMe	52.9	53.2[c]	53.1[d]	53.2	53.3[e]	53.3[f]	54.5	54.5	54.6	52.8	53.2[h]	53.0[k]	53.1[l]	53.2[m]	53.2[i]	53.1[j]
NCO_2Me	53.4	53.4[c]	53.5[d]	53.5	53.5[e]	53.6[f]	—	—	—	53.0	53.4[h]	53.2[k]	52.9[l]	53.5[m]	53.4[i]	53.5[j]
NCO_2Me	155.4	154.4	154.3	[b]	155.5	[b]	—	—	—	155.6	[b]	156.9	155.6	[b]	[b]	154.5
OCH_2O	101.1	101.1	101.2	101.1	101.2	101.2	—	—	—	101.1	101.0	—	—	101.1	101.2	101.1
11-OMe	—	—	—	—	—	—	—	57.2	—	—	—	—	—	—	—	—
12-OMe	—	—	—	—	—	—	—	—	—	—	—	56.2	56.4	—	—	—
NCO_2	—	—	—	—	—	—	152.1	151.8	151.5	—	—	—	—	—	—	—

[a] $CDCl_3$, 100 MHz; assignments based on HMQC and HMBC.
[b] Not detected.
[c–m] Assignments may be reversed.

The mersidasines (**11**–**17**) are characterized by additional hydroxyl substitution on the piperidine ring D. Mersidasine A (**11**) was obtained as a light yellowish oil with $[\alpha]_D$ −6 (*c* 0.41, $CHCl_3$). The UV (211, 236, and 286 nm) and IR spectra (3471, 1740, and 1712 cm^{-1}) were similar to those of the mersinines, indicating the presence of similar chromophore and functionalities (OH, ester, and carbamate/ester functions) in mersidasine A (**11**). The EIMS showed a molecular ion at *m/z* 518, which analyzed for $C_{25}H_{30}N_2O_{10}$, differing from the mersinines (**1**–**3**) by 18 mass units (or addition of H and OH). The ^1H NMR spectral data (Table 2) showed a general similarity with those of mersinine A (**1**), except for the absence of the 14,15-olefinic H resonances. The ^{13}C NMR spectrum (Table 3) gave a total of 25 separate carbon resonances (three methyls, seven methylenes, five methines, and 10 quaternary carbons) in agreement with the molecular formula. The spectrum also indicated the absence of the two olefinic methine carbon resonances, which have been replaced by a methylene (δ 32.3) and an oxymethine resonance (δ 69.3) when compared to **1**. These differences were also reflected in the COSY spectrum of **11**, which indicated replacement of an $NCH_2CH{=}CH$ fragment by an NCH_2CH_2CHOH fragment compared to **1**. These differences suggested the presence in **11** of a similar ring system compared to **1**, with the major change being the replacement of the 14,15-unsaturation by a hydroxy substituent at C-15. The position of OH substitution was further confirmed from the HMBC data, which showed correlations from H-3 and H-21 to C-15, and from H-15 to C-3, C-21 and C-17. The C(16)–OH signal was observed at δ 4.65, while the C-2 resonance was observed at δ 52.9, features which are diagnostic of an (*R*) configuration at the quaternary C-16, as was the relative deshielding of H-18α versus H-18β. The NMR spectral data, as well as the observed H-9/H-21, H-2/H-21, H-21/H-19α, and H-2/H-19α NOEs, were similar to those seen in **1** and indicated similar relative configurations at C-7, C-21, C-2, and C-20. It remained to determine the stereochemistry of the C(15)–OH group, which was deduced to be α from the observed NOE between H-19β and H-15.

Mersidasine B (**12**) was obtained as a colorless amorphous solid with $[\alpha]_D$ −7 (*c* 0.47, $CHCl_3$). The UV spectrum was generally similar to that of mersidasine A (**11**) and the IR spectrum indicated the presence of similar functionalities (OH, ester, and carbamate groups). The EIMS showed the same molecular ion (*m/z* 518) indicating that **11** and **12** are isomers. The ^1H and ^{13}C NMR spectral data of **12** (Tables 2 and 3) were also essentially similar to those of **11**, except for minor variations in the chemical shifts. The major differences were in the shifts of C(16)–OH (δ 5.11 vs 4.65) and C-2 (δ 49.4 vs 53.1), which indicated that **12** differed from **11** in the configuration of the quaternary C-16, which from the diagnostic shift values was deduced to be (*S*). The stereochemistry of the C(15)–OH group is also α from the observed NOE between H-19β and H-15. Mersidasine B (**12**) is therefore the 16(*S*) epimer of mersidasine A (**11**).

Mersidasine C (**13**) was obtained as a light yellowish oil with $[\alpha]_D$ +23 (*c* 0.22, $CHCl_3$). The UV spectrum was similar to that of the other mersidasine compounds while the IR spectrum indicated the presence of OH, ester, and carbamate functionalities. The EIMS showed a molecular ion at *m/z* 504, which analyzed for $C_{25}H_{32}N_2O_9$. Examination of the NMR spectral data (Tables 2 and 3) indicated a similarity with mersidasine A (**11**) except for a difference in aromatic substitution. The ^1H NMR spectrum (Table 2) showed the presence of three contiguous aromatic hydrogens. The observed H-21/H-9 NOE, coupled with the presence of an additional aromatic methoxy substituent (δ_H 3.86; δ_C 56.2), indicated substitution at C-12 by a methoxy group. The NMR and NOE/NOESY data were also similar to those obtained for mersidasine A (**11**), confirming the same relative configurations at C-7, C-21, C-2, C-20, and C-15. The characteristic C(16)–OH and C-2 shifts of δ 4.57 and 53.6, respectively, were similar to those of mersidasine A (**11**) (δ 4.65 and 53.1, respectively), indicating that **11** and **13** have the same 16(*R*) configuration.

Mersidasine D (**14**) was obtained as a colorless oil with $[\alpha]_D$ −20 (*c* 0.12, $CHCl_3$). The UV, IR, MS, and NMR data were very similar to those of mersidasine C (**13**) indicating a similar structure with C(12)–OMe and C(15)–αOH groups. The major difference was in the configuration at the quaternary C-16, which was deduced to be *S* from the characteristic C(16)–OH and C-2 shifts of δ 5.21 and 49.6, respectively (compared to δ 4.57 and 53.6, respectively, in mersidasine C (**13**)). Mersidasine D (**14**) is therefore the 16(*S*) epimer of mersidasine C (**13**).

Mersidasine E (**15**) was obtained as a light yellowish oil with $[\alpha]_D$ −7 (*c* 0.37, $CHCl_3$). The UV and IR spectra were essentially similar to those of the previous mersidasine compounds. The EIMS showed a molecular ion at *m/z* 534, which analyzed for $C_{25}H_{30}N_2O_{11}$, differing from mersidasines A and B (**11** and **12**) by 16 mass units, or, replacement of H by OH. The NMR spectral data (Tables 2 and 3) were rather similar to those of mersidasines B (**12**) and D (**14**), except for changes in the piperidine ring D, which has incorporated a 1,2-diol function, as evident from the presence of two oxymethines (δ_H 3.34, 3.91; δ_C 69.3, 81.6) as well as from the COSY spectrum, which indicated the presence of an $NCH_2CH(OH)$-$CH(OH)$ fragment. This constitutes the major difference between **15** versus **12** and **14**. The NOE/NOESY data were similar to those observed for mersidasines B (**12**) and D (**14**), as were the characteristic C(16)–OH and C-2 shifts (δ 5.13 and 48.7, respectively), which indicated a common relative configuration at all the asymmetric centers. The main difference is therefore the presence of a 1,2-diol in place of a C(15)–OH in the piperidine ring. The stereochemistry at C-14 and C-15 can be readily inferred from the NOE data. The NOEs observed between H-15/H-21 and H-15/H-19α indicate that the H-15 stereochemistry is α, while the absence of any NOE between H-15 and H-14 indicates that the stereochemistry of H-14 is β. The stereochemistry of the C(14)– and C(15)–OH groups are therefore α and β, respectively. The configuration at C-16 is (*S*) from the observed C(16)–OH and C-2 shifts of δ 5.13 and 48.7, respectively, which were similar to those of mersidasines B (**12**) and D (**14**).

Mersidasine F (**16**) was obtained as a colorless oil with $[\alpha]_D$ +33 (*c* 0.15, $CHCl_3$). The UV spectrum was generally similar

to that of mersidasines A (**11**) and B (**12**), as was the IR spectrum, which showed the presence of similar functionalities (OH, ester, and carbamate). However, in common with mersinine C (**3**) and mersifoline C (**10**), Wenkert–Bohlmann bands (2798, 2901 cm^{-1}) were observed in **16**, which were not seen in **11** and **12**, indicating a trans-D/E ring junction, similar to those seen in mersinine C (**3**) and mersifoline C (**10**). The EIMS showed the same molecular ion (*m/z* 518) indicating that all three compounds (**16**, **12**, **11**) are isomers. In common with **11** and **12**, the NMR spectral data of **16** (Tables 2 and 3) showed the presence of a similar quinolinic, pentacyclic, carbon skeleton, with a methylenedioxy group, carbamate, a quaternary C(16) linked to OH and methyl ester groups, a methyl ester substituent at C-20, and an OH substituent at C-15. The NMR and NOE/NOESY data obtained (NOEs for H-9/H-21, H-18β/H-6β, H-3α/H-21 seen; NOEs for H-21/H-19α, H-21/H-2, H-2/H-19α not seen) were similar to those observed in mersinine C (**3**) and mersifoline C (**10**), which provided further confirmation for the trans-D/E ring junction as well as the *R* configuration at C-20 (C(20)–αCO_2Me). The C(16)–OH (δ 4.42) and C-2 (δ 49.1) shifts in this case have to be compared with those of mersidasine G (**17**), which also possesses the same trans-D/E ring junction as well as 20(*R*) configuration (δ 5.13 and 44.5, respectively, vide infra), from which it can be inferred that the configuration at C-16 is *R* (the C-2 shifts of the 16(*R*) epimers in the mersinine-type compounds are consistently shifted downfield by ca. 4 ppm compared to the corresponding 16(*S*) epimers, vide supra). As in the previous compounds, the stereochemistry of the C(15)–OH group was deduced to be α from the observed NOE between H-15 and H-19β. Mersidasine F (**16**) is therefore the 20(*R*) epimer of mersidasine A (**11**).

Mersidasine G (**17**) was obtained as a colorless oil with $[\alpha]_D$ −30 (*c* 0.33, $CHCl_3$). The UV, IR, MS, and NMR data were very similar to those of mersidasine C (**13**). The presence of Wenkert–Bohlmann bands (2798, 2890 cm^{-1}), coupled with the similar NMR and NOE/NOESY data (NOEs for H-9/H-21, H-18β/H-6β, H-3α/H-21 seen; NOEs for H-21/H-19α, H-21/H-2, H-2/H-19α not seen), indicated the presence of the same trans-D/E ring junction as well as the *R* configuration at C-20 (C(20)–αCO_2Me). The observed H-15/H-19α NOE confirmed that the stereochemistry of the C(15)–OH was unchanged compared with **13**. Comparison of the diagnostic C(16)–OH and C-2 shifts, δ 5.13 and 44.5, respectively, with the corresponding shifts in mersidasine C (**13**), δ 4.42 and 49.1, respectively, allowed the configuration at C-16 to be deduced as *S*. Mersidasine G (**17**) is therefore the 20(*R*) epimer of mersidasine B (**12**).

Analysis of the coupling behavior of the ring D hydrogens (Table 2) as well as the NOE data revealed another additional feature in the mersidasine group of compounds. It can be seen that those compounds with a cis-D/E ring junction and C(20*S*) configuration (or C(20)–βCO_2Me), i.e., mersidasines A, B, C, and D, the coupling behavior of H-14 and H-15 ($J_{14\beta-15}$=7.5; $J_{14\beta-3\alpha}$=$J_{14\beta-3\beta}$=4) coupled with the observed H-21/H-14α NOE suggest that in these compounds, the conformation preferred by the piperidine ring D is boat (or twist-boat), whereas in mersidasines F and G, which have a trans-D/E ring junction and 20(*R*) configuration (C(20)–αCO_2Me), the observed H-21/H-3α NOE indicates that it is the chair conformation that is preferred. Another trend observed concerns the shift of the 17-OMe (ester) group. In compounds with cis-D/E ring junction and C(20)–βCO_2Me (e.g., **1**–**2**, **4**–**9**, **11**–**15**), the 17-OMe is observed at ca. δ 3.6, whereas in compounds with trans-D/E ring junction and C(20)–αCO_2Me (e.g., **3**, **10**, **16**, **17**), the 17-OMe signal is shifted slightly upfield to ca. δ 3.4 (Tables 1 and 2).

The transformation of mersinine A to its thermodynamically more stable epimer mersinine B by an irreversible base-induced epimerization has been noted earlier. This observation in turn raises the possibility that some of the C-16 epimers may be artefacts of the isolation procedure, although the mild conditions under which extraction of the alkaloids was carried out render this unlikely. Moreover the alkaloids do not epimerize during TLC. Nevertheless, in order to rule out the possibility that the stable epimers are artefacts, control experiments were carried out in which the alkaloids were redissolved in dilute acid, followed by basification with concentrated ammonia to release the alkaloids, which were then taken into chloroform and examined by TLC. It was found that in the case of mersinine A, mersiloscine A, mersidasine C, and mersidasine F, the alkaloids were in the main recovered intact, although traces of the C-16 epimers were also detected. These observations, therefore, indicate that epimerization at C-16 during isolation may account partially, though not entirely, for the presence of these alkaloids in the basic fraction.

All 16 alkaloids did not show any appreciable cytoxicity when tested against KB cells (IC_{50}>25 μg/mL). Mersinines A (**1**), B (**2**), C (**3**), and mersifolines B (**9**) and C (**10**), however, were found to reverse drug-resistance in drug-resistant KB (KB/VJ300) cells (Table 4), while the mersiloscines

Table 4
Cytotoxic effects of **1**–**6** and **9**–**17**

Compound	IC_{50}, μg/mL (μM)		
	KB/S[a]	KB/VJ300[a]	KB/VJ300[b,c]
Mersinine A (**1**)	>25	>25	4.1 (8.2)
Mersinine B (**2**)	>25	>25	3.2 (8.4)
Mersinine C (**3**)	>25	>25	11.2 (22.4)
Mersifoline B (**9**)	>25	>25	3.7 (7.9)
Mersifoline C (**10**)	>25	>25	7 (15.9)
Mersiloscine (**4**)	>25	>25	>25
Mersiloscine A (**5**)	>25	>25	>25
Mersiloscine B (**6**)	>25	>25	>25
Mersidasine A (**11**)	>25	>25	>25
Mersidasine B (**12**)	>25	>25	>25
Mersidasine C (**13**)	>25	>25	>25
Mersidasine D (**14**)	>25	>25	>25
Mersidasine E (**15**)	>25	>25	>25
Mersidasine F (**16**)	>25	>25	>25
Mersidasine G (**17**)	>25	>25	>25

[a] KB/S and KB/VJ300 are vincristine-sensitive and -resistant human oral epidermoid carcinoma cell lines, respectively.

[b] With added vincristine 0.1 μg/mL (0.12 μM), which did not affect the growth of the KB/VJ300 cells.

[c] The IC_{50} values of vincristine against KB/S and KB/VJ300 strains are 0.0023 and 1.0 μg/mL (0.0028 and 1.2 μM), respectively.

(**4**–**6**) and the mersidasines (**11**–**17**), which are characterized by the presence of a C(15)–OH substituent (as well as an additional lactone ring in the case of the mersiloscines), were found to be ineffective (IC_{50}>25 μg/mL).[13] Among the active compounds, the stereoisomer with trans-D/E ring junction and C(20)–αCO_2Me appear to be less effective compared to that with cis-D/E ring junction and C(20)–βCO_2Me (cf **1**, **2** vs **3**; **9** vs **10**). In any case, these alkaloids represent the first members of a new structural subclass of the monoterpenoid indoles, and are found exclusively and for the first time from the same plant.

3. Experimental

3.1. General

Optical rotations were determined on a JASCO DIP-370 digital polarimeter or on an Atago Polax-D polarimeter. IR spectra were recorded on a Perkin–Elmer RX1 FT-IR spectrophotometer. UV spectra were obtained on a Shimadzu UV-3101PC spectrophotometer. ^{1}H and ^{13}C NMR spectra were recorded in $CDCl_3$ using TMS as internal standard on a JEOL JNM-LA 400 spectrometer at 400 and 100 MHz, respectively. EIMS and HREIMS were obtained at Organic Mass Spectrometry, Central Science Laboratory, University of Tasmania, Tasmania, Australia.

3.2. Plant material

Plant material was collected in Johor, Malaysia and was identified by Dr. D. J. Middleton, Rijks Herbarium, University of Leiden, Leiden, The Netherlands (present address: Royal Botanic Garden, 20A Inverleith Row, Edinburgh, Scotland).[22,23] Herbarium voucher specimens (K649, K657) are deposited at the Herbarium of the University of Malaya and at Leiden.

3.3. Extraction and isolation

Extraction of the ground leaf material was carried out in the usual manner by partitioning the concentrated EtOH extract with dilute acid as has been described in detail elsewhere.[18] The alkaloids were isolated by initial column chromatography on silica gel using $CHCl_3$ with increasing proportions of MeOH followed by rechromatography of appropriate partially resolved fractions using centrifugal TLC. Solvent systems used for centrifugal TLC were Et_2O, Et_2O/hexane (1:1), Et_2O/hexane (1:2), Et_2O/hexane (2:1), Et_2O/MeOH (100:1), Et_2O/MeOH (50:1), EtOAc, EtOAc/MeOH (50:1), EtOAc/MeOH (30:1), $CHCl_3$, $CHCl_3$/MeOH (100:1), and $CHCl_3$/MeOH (50:1). The yields (g kg^{-1}) of the alkaloids were as follows: **1** (0.011), **2** (0.044), **3** (0.048), **4** (0.014), **5** (0.013), **6** (0.017), **8** (0.005), **9** (0.005), **10** (0.003), **11** (0.008), **12** (0.059), **13** (0.004), **14** (0.003), **15** (0.007), **16** (0.003), and **17** (0.006).

3.3.1. Mersinine A (*1*)

Colorless crystals from ether; mp 204–205 °C; $[\alpha]_D$ −58 (*c* 0.27, $CHCl_3$); UV (EtOH) λ_{max} nm (log ε) 213 (4.50), 239 (4.10), 289 (3.82); IR (dry film) ν_{max} 3523, 1739, 1684 cm^{-1}; EIMS *m/z* (rel int) 500 $[M]^+$ (87), 485 (15), 441 (100), 409 (36), 381 (32), 352 (19), 321 (15), 293 (13), 151 (21), 149 (7); HREIMS *m/z* 500.1798 (calcd for $C_{25}H_{28}N_2O_9$ $[M]^+$, 500.1795); ^{1}H NMR (400 MHz, $CDCl_3$), see Table 1; ^{13}C NMR (100 MHz, $CDCl_3$), see Table 3.

3.3.2. Mersinine B (*2*)

Colorless oil; $[\alpha]_D$ −77 (*c* 0.48, $CHCl_3$); UV (EtOH) λ_{max} nm (log ε) 214 (4.55), 241 (4.17), 287 (3.79); IR (dry film) ν_{max} 3506, 1748, 1709 cm^{-1}; EIMS *m/z* (rel int) 500 $[M]^+$ (64), 485 (19), 441 (100), 409 (12), 381 (11), 352 (8), 321 (5), 293 (13), 151 (8), 149 (34); HREIMS *m/z* 500.1798 (calcd for $C_{25}H_{28}N_2O_9$ $[M]^+$, 500.1795); ^{1}H NMR (400 MHz, $CDCl_3$), see Table 1; ^{13}C NMR (100 MHz, $CDCl_3$), see Table 3.

3.3.3. Mersinine C (*3*)

Colorless crystals from ether; mp 108–110 °C; $[\alpha]_D$ +14 (*c* 0.72, $CHCl_3$); UV (EtOH) λ_{max} nm (log ε) 217 (4.46), 244 (3.99), 288 (3.46); IR (dry film) ν_{max} 3495, 1745, 1728 cm^{-1}; EIMS *m/z* (rel int) 500 $[M]^+$ (88), 485 (13), 441 (100), 427 (18), 409 (29), 381 (11), 321 (6), 293 (6), 218 (6), 151 (7); HREIMS *m/z* 500.1800 (calcd for $C_{25}H_{28}N_2O_9$ $[M]^+$, 500.1795); ^{1}H NMR (400 MHz, $CDCl_3$), see Table 1; ^{13}C NMR (100 MHz, $CDCl_3$), see Table 3.

3.3.4. Mersiloscine (*4*)

Colorless amorphous solid; mp 185–188 °C; $[\alpha]_D$ −50 (*c* 0.04, $CHCl_3$); UV (EtOH) λ_{max} nm (log ε) 215 (4.53), 242 (4.09), 291 (3.55); IR (dry film) ν_{max} 3484, 1749, 1700 cm^{-1}; EIMS *m/z* (rel int) 502 $[M]^+$ (39), 443 (100), 411 (28), 383 (39), 329 (3), 275 (5), 219 (4); HREIMS *m/z* 502.1590 (calcd for $C_{24}H_{26}N_2O_{10}$ $[M]^+$, 502.1587); ^{1}H NMR (400 MHz, $CDCl_3$), see Table 1; ^{13}C NMR (100 MHz, $CDCl_3$), see Table 3.

3.3.5. Mersiloscine A (*5*)

Colorless oil; $[\alpha]_D$ −38 (*c* 0.66, $CHCl_3$); UV (EtOH) λ_{max} nm (log ε) 213 (4.53), 235 (4.17), 289 (3.66); IR (dry film) ν_{max} 3468, 1751, 1707 cm^{-1}; EIMS *m/z* (rel int) 502 $[M]^+$ (100), 443 (84), 429 (26), 425 (31), 411 (42), 387 (34), 383 (35), 220 (21), 149 (32); HREIMS *m/z* 502.1586 (calcd for $C_{24}H_{26}N_2O_{10}$ $[M]^+$, 502.1587); ^{1}H NMR (400 MHz, $CDCl_3$), see Table 1; ^{13}C NMR (100 MHz, $CDCl_3$), see Table 3.

3.3.6. Mersiloscine B (*6*)

Colorless amorphous solid; mp 202–204 °C; $[\alpha]_D$ +24 (*c* 0.20, $CHCl_3$); UV (EtOH) λ_{max} nm (log ε) 212 (3.93), 244 (3.44), 287 (2.98); IR (dry film) ν_{max} 3484, 1748, 1706 cm^{-1}; EIMS *m/z* (rel int) 502 $[M]^+$ (35), 488 (23), 459 (17), 443 (100), 429 (41), 411 (31), 383 (35), 369 (19), 297 (48), 268 (19), 167 (24), 150 (33), 127 (24), 109 (25); HREIMS *m/z* 502.1594 (calcd for $C_{24}H_{26}N_2O_{10}$ $[M]^+$,

502.1587); ^{1}H NMR (400 MHz, $CDCl_3$), see Table 1; ^{13}C NMR (100 MHz, $CDCl_3$), see Table 3.

3.3.7. Mersifoline A (**8**)

Colorless oil; $[\alpha]_D$ −19 (*c* 0.26, $CHCl_3$); UV (EtOH) λ_{max} nm (log ε) 206 (4.02), 230 (3.36), 271 (3.00); IR (dry film) ν_{max} 3434, 1784, 1738 cm^{-1}; EIMS *m/z* (rel int) 440 $[M]^+$ (38), 425 (19), 381 (100), 353 (9), 321 (13), 293 (12), 265 (7), 226 (13), 205 (7), 167 (9), 151 (14), 109 (17); HREIMS *m/z* 440.1586 (calcd for $C_{23}H_{24}N_2O_7$ $[M]^+$, 440.1584); ^{1}H NMR (400 MHz, $CDCl_3$), see Table 1; ^{13}C NMR (100 MHz, $CDCl_3$), see Table 3.

3.3.8. Mersifoline B (**9**)

Colorless oil; $[\alpha]_D$ −14 (*c* 0.18, $CHCl_3$); UV (EtOH) λ_{max} nm (log ε) 211 (4.40), 229 (4.05), 270 (3.52); IR (dry film) ν_{max} 3463, 1781, 1735 cm^{-1}; EIMS *m/z* (rel int) 470 $[M]^+$ (45), 455 (24), 411 (100), 381 (13), 351 (15), 323 (13), 281 (10), 252 (8), 218 (16), 191 (10), 167 (18), 149 (23); HREIMS *m/z* 470.1695 (calcd for $C_{24}H_{26}N_2O_8$ $[M]^+$, 470.1689); ^{1}H NMR (400 MHz, $CDCl_3$), see Table 1; ^{13}C NMR (100 MHz, $CDCl_3$), see Table 3.

3.3.9. Mersifoline C (**10**)

Colorless oil; $[\alpha]_D$ +18 (*c* 0.28, $CHCl_3$); UV (EtOH) λ_{max} nm (log ε) 211 (3.84), 230 (3.72), 273 (3.30); IR (dry film) ν_{max} 3468, 1784, 1752, 1728 cm^{-1}; EIMS *m/z* (rel int) 440 $[M]^+$ (38), 425 (18), 381 (100), 321 (16), 293 (9), 265 (5), 151 (11); HREIMS *m/z* 440.1591 (calcd for $C_{23}H_{24}N_2O_7$ $[M]^+$, 440.1584); ^{1}H NMR (400 MHz, $CDCl_3$), see Table 2; ^{13}C NMR (100 MHz, $CDCl_3$), see Table 3.

3.3.10. Mersidasine A (**11**)

Light yellowish oil; $[\alpha]_D$ −6 (*c* 0.41, $CHCl_3$); UV (EtOH) λ_{max} nm (log ε) 211 (4.35), 236 (3.96), 286 (3.46); IR (dry film) ν_{max} 3471, 1740, 1712 cm^{-1}; EIMS *m/z* (rel int) 518 $[M]^+$ (13), 500 (39), 459 (26), 441 (100), 427 (7), 409 (10), 381 (11), 353 (5), 275 (4), 236 (3), 151 (4); HRMS *m/z* 518.1893 (calcd for $C_{25}H_{30}N_2O_{10}$ $[M]^+$, 518.1900); ^{1}H NMR (400 MHz, $CDCl_3$), see Table 2; ^{13}C NMR (100 MHz, $CDCl_3$), see Table 3.

3.3.11. Mersidasine B (**12**)

Colorless amorphous solid; mp 215–217 °C; $[\alpha]_D$ −7 (*c* 0.47, $CHCl_3$); UV (EtOH) λ_{max} nm (log ε) 214 (4.00), 240 (3.60), 287 (3.04), 293 (3.07); IR (dry film) ν_{max} 3504, 1741, 1702 cm^{-1}; EIMS *m/z* (rel int) 518 $[M]^+$ (53), 500 (53), 459 (94), 441 (100), 427 (28), 409 (18), 381 (14), 275 (8), 236 (10), 205 (28); HRFABMS *m/z* 519.1981 (calcd for $C_{25}H_{31}N_2O_{10}$ $[MH]^+$, 519.1979); ^{1}H NMR (400 MHz, $CDCl_3$), see Table 2; ^{13}C NMR (100 MHz, $CDCl_3$), see Table 3.

3.3.12. Mersidasine C (**13**)

Light yellowish oil; $[\alpha]_D$ +23 (*c* 0.22, $CHCl_3$); UV (EtOH) λ_{max} nm (log ε) 209 (4.31), 234 (3.73), 284 (3.17); IR (dry film) ν_{max} 3482, 1740, 1707 cm^{-1}; EIMS *m/z* (rel int) 504 $[M]^+$ (6), 486 (26), 468 (11), 445 (14), 427 (100), 409 (30), 367 (17), 349 (11), 307 (10), 261 (8), 197 (9), 167 (11), 149 (15); HREIMS *m/z* 504.2109 (calcd for $C_{25}H_{32}N_2O_9$ $[M]^+$, 504.2108); ^{1}H NMR (400 MHz, $CDCl_3$), see Table 2; ^{13}C NMR (100 MHz, $CDCl_3$), see Table 3.

3.3.13. Mersidasine D (**14**)

Colorless oil; $[\alpha]_D$ −205 (*c* 0.12, $CHCl_3$); UV (EtOH) λ_{max} nm (log ε) 218 (4.23), 244 (3.73), 284 (3.01); IR (dry film) ν_{max} 3502, 1740, 1700 cm^{-1}; EIMS *m/z* (rel int) 504 $[M]^+$ (53), 500 (53), 459 (94), 441 (100), 427 (28), 409 (18), 381 (14), 275 (8), 236 (10), 205 (28); HREIMS *m/z* 504.2092 (calcd for $C_{25}H_{32}N_2O_9$ $[M]^+$, 504.2108); ^{1}H NMR (400 MHz, $CDCl_3$), see Table 2; ^{13}C NMR (100 MHz, $CDCl_3$), see Table 3.

3.3.14. Mersidasine E (**15**)

Light yellowish oil; $[\alpha]_D$ −7 (*c* 0.37, $CHCl_3$); UV (EtOH) λ_{max} nm (log ε) 213 (4.63), 239 (4.25), 287 (3.76); IR (dry film) ν_{max} 3471, 1746, 1721, 1711 cm^{-1}; EIMS *m/z* (rel int) 534 $[M]^+$ (24), 505 (16), 475 (100), 443 (39), 429 (18), 399 (15), 369 (7), 300 (7), 275 (15), 243 (14), 188 (10), 130 (5); HREIMS *m/z* 534.1841 (calcd for $C_{25}H_{30}N_2O_{11}$ $[M]^+$, 534.1850); ^{1}H NMR (400 MHz, $CDCl_3$), see Table 2; ^{13}C NMR (100 MHz, $CDCl_3$), see Table 3.

3.3.15. Mersidasine F (**16**)

Colorless oil; $[\alpha]_D$ +33 (*c* 0.15, $CHCl_3$); UV (EtOH) λ_{max} nm (log ε) 213 (4.18), 237 (3.75), 290 (3.25); IR (dry film) ν_{max} 3485, 2901, 2798, 1742, 1714 cm^{-1}; EIMS *m/z* (rel int) 518 $[M]^+$ (53), 500 (53), 459 (94), 441 (100), 427 (28), 409 (18), 381 (14), 275 (8), 236 (10), 205 (28); HREIMS *m/z* 518.1897 (calcd for $C_{25}H_{30}N_2O_{10}$ $[M]^+$, 518.1900); ^{1}H NMR (400 MHz, $CDCl_3$), see Table 2; ^{13}C NMR (100 MHz, $CDCl_3$), see Table 3.

3.3.16. Mersidasine G (**17**)

Colorless oil; $[\alpha]_D$ −30 (*c* 0.33, $CHCl_3$); UV (EtOH) λ_{max} nm (log ε) 217 (4.33), 240 (3.94), 288 (3.39); IR (dry film) ν_{max} 3492, 3356, 2890, 2798, 1745, 1714 cm^{-1}; EIMS *m/z* (rel int) 518 $[M]^+$ (53), 500 (53), 459 (94), 441 (100), 427 (28), 409 (18), 381 (14), 275 (8), 236 (10), 205 (28); HREIMS *m/z* 518.1914 (calcd for $C_{25}H_{30}N_2O_{10}$ $[M]^+$, 518.1900); ^{1}H NMR (400 MHz, $CDCl_3$), see Table 2; ^{13}C NMR (100 MHz, $CDCl_3$), see Table 3.

Acknowledgements

We would like to thank the University of Malaya and MOSTI Malaysia (ScienceFund) for financial support.

References and notes

1. Lim, K. H.; Komiyama, K.; Kam, T. S. *Tetrahedron Lett.* **2007**, *48*, 1143.
2. Lim, K. H.; Kam, T. S. *Helv. Chim. Acta* **2007**, *90*, 31.
3. Lim, K. H.; Kam, T. S. *Tetrahedron Lett.* **2006**, *47*, 8653.
4. Lim, K. H.; Kam, T. S. *Org. Lett.* **2006**, *8*, 1733.
5. Lim, K. H.; Low, Y. Y.; Kam, T. S. *Tetrahedron Lett.* **2006**, *47*, 5037.
6. Kam, T. S.; Subramaniam, G.; Lim, K. H.; Choo, Y. M. *Tetrahedron Lett.* **2004**, *45*, 5995.

7. Kam, T. S.; Subramaniam, G. *Tetrahedron Lett*. **2004**, *45*, 3521.
8. Kam, T. S.; Choo, Y. M. *Helv. Chim. Acta* **2004**, *87*, 991.
9. Kam, T. S.; Choo, Y. M. *Tetrahedron Lett*. **2003**, *44*, 1317.
10. Kam, T. S.; Subramaniam, G.; Lim, T. M. *Tetrahedron Lett*. **2001**, *42*, 5977.
11. Kam, T. S.; Lim, T. M.; Choo, Y. M. *Tetrahedron* **1999**, *55*, 1457.
12. Kam, T. S. *Alkaloids: Chemical and Biological Perspectives*; Pelletier, S. W., Ed.; Pergamon: Amsterdam, 1999; Vol. 14, pp 285–435.
13. Kam, T. S.; Subramaniam, G.; Sim, K. M.; Yoganathan, K.; Koyano, T.; Toyoshima, M.; Rho, M. C.; Hayashi, M.; Komiyama, K. *Bioorg. Med. Chem. Lett*. **1998**, *8*, 2769.
14. Kam, T. S.; Yoganathan, K.; Chen, W. *Tetrahedron Lett*. **1996**, *37*, 3603.
15. Kam, T. S.; Yoganathan, K.; Koyano, T.; Komiyama, K. *Tetrahedron Lett*. **1996**, *37*, 5765.
16. Kam, T. S.; Yoganathan, K.; Chuah, C. H. *Tetrahedron Lett*. **1995**, *36*, 759.
17. Kam, T. S.; Yoganathan, K.; Chuah, C. H. *Tetrahedron Lett*. **1994**, *35*, 4457.
18. Kam, T. S.; Yoganathan, K.; Chuah, C. H. *Tetrahedron Lett*. **1993**, *34*, 1819.
19. Kam, T. S.; Lim, T. M.; Tan, G. H. *J. Chem. Soc., Perkin Trans. 1* **2001**, 1594.
20. Uzir, S.; Mustapha, A. M.; Hadi, A. H. A.; Awang, K.; Wiart, C.; Gallard, J. F.; Pais, M. *Tetrahedron Lett*. **1997**, *38*, 1571.
21. Awang, K.; Sevenet, T.; Hadi, A. H. A.; David, B.; Pais, M. *Tetrahedron Lett*. **1992**, *33*, 2493.
22. The plant was tentatively identified by Dr. David Middleton as *Kopsia fruticosa* in the first instance (Ref. 10), but was amended to *K. singapurensis* on completion of his review of the genus *Kopsia* (following reference).
23. Middleton, D. J. *Harv. Pap. Bot*. **2004**, *9*, 89.
24. Hugel, G.; Levy, J. *J. Org. Chem*. **1986**, *51*, 1594.
25. Hugel, G.; Levy, J. *J. Org. Chem*. **1984**, *49*, 3275.
26. Kam, T. S.; Sim, K. M.; Lim, T. M. *Tetrahedron Lett*. **2001**, *42*, 4721.
27. Bisset, N. G.; Das, B. C.; Parello, J. *Tetrahedron* **1973**, *29*, 4137.
28. Subramaniam, G.; Kam, T. S.; Ng, S. W. *Acta Crystallogr*. **2003**, *E59*, o555.
29. Rosen, W. E. *Tetrahedron Lett*. **1961**, 481.
30. Wenkert, E.; Guo, M.; Pestchanker, M. J.; Shi, Y. J.; Vankar, Y. T. *J. Org. Chem*. **1989**, *54*, 1166.
31. Richardson, A., Jr. *J. Org. Chem*. **1963**, *28*, 2581.